Metal-insulator transitions in Ti_4O_7 single crystals: Crystal characterization, specific heat, and electron paramagnetic resonance*†

S. Lakkis, C. Schlenker, B. K. Chakraverty, and R. Buder
Groupe des Transitions de Phases, Centre National de la Recherche Scientifique, 166 X, 38042 Grenoble, France

M. Marezio
Laboratoire des Rayons X, Centre National de la Recherche Scientifique, 166 X, 38042 Grenoble, France
(Received 6 October 1975)

Ti_4O_7 single crystals have been studied by different methods in order to elucidate the nature of the three phases and the mechanisms of the two successive metal-insulator transitions. The crystals have been characterized by x-ray diffraction methods together with electron-paramagnetic-resonance (EPR) studies. Heat-capacity and entropy changes at the transition have been measured. On the basis of these data and of previous results, it is proposed that the low-temperature transition is related to a *disordering of the* Ti^{3+} *pairs*. While in the low-temperature phase, Ti chains are alternatively occupied by Ti^{4+} ions and Ti^{3+} pairs, Ti^{3+} pairing also occurs in the intermediate phase but without any long-range order. A detailed model of disordered chains is given. Good agreement is found between the calculated and experimental values of the entropy change. It is also shown from both magnetic-susceptibility and specific-heat data, that for the high-temperature transition, the lattice contribution to the entropy is of the same order of magnitude as the electronic one. EPR spectra have been studied on untwinned crystals. A Ti^{3+} center, attributed to a stoichiometry defect has been identified through the ^{47}Ti-^{49}Ti hyperfine structure. The intensity of the line follows a Curie-Weiss law at low temperature and decreases sharply at the low-temperature transition. The vanishing of this line in the intermediate phase shows that the disorder of this phase is *dynamic*. The linewidth increase below the transition is attributed to a multiphonon Orbach relaxation through empty Ti^{4+} levels. The nature of the three phases of Ti_4O_7 is discussed. The low-temperature phase may be described by an order of the Verwey type for the Ti^{3+} pairs. Interchain electronic correlations are shown to be the dominant mechanism responsible for this order. An atomic level scheme is given for this phase. *Bipolarons* are shown to be responsible for the transport properties in the intermediate phase and the bipolaronic state is discussed. In the metallic phase, the high Pauli magnetic susceptibility is attributed to an enhancement due to the interatomic electronic correlations.

I. INTRODUCTION

Titanium oxide (Ti_4O_7) belongs to the class of material, including mainly titanium and vanadium compounds, which show temperature-induced metal-insulator transitions.[1-3] It is a member of the homologous series Ti_nO_{2n-1} known as Magneli phases.[4] Unlike the sesquioxide Ti_2O_3, which has only one valence state (Ti^{3+}), Ti_4O_7 is a mixed-valence compound with as many 3^+ ($3d^1$ electronic configuration) as 4^+ states. This feature might be responsible for uncommon properties such as the existence of two phase transitions and of three well-differentiated phases.

The electrical resistivity, magnetic susceptibility, and crystal structure have been investigated previously. Ti_4O_7 shows two conductivity transitions, a semiconductor-semiconductor one in the temperature range of 130–140 K and a semiconductor-metal one at 150 K.[5] For both transitions, there is a steep increase of the electrical conductivity with increasing temperature. The magnetic susceptibility is small and temperature independent below 150 K, shows a sharp enhancement at 150 K, and does not show any anomaly at 140 K.[6] A decrease of the unit-cell volume is also observed at 150 K.[7]

The crystal structure of the Magneli phases Ti_nO_{2n-1} is related to that of rutile TiO_2 and consists of rutilelike blocks which are infinite in two dimensions and n oxygen-octahedra wide in the third.[8] Along the plane separating these blocks [$(1\ \bar{2}\ 1)$ of rutile], the octahedra share faces, edges, and corners, while inside the blocks they share only edges and corners. The anion packing remains essentially close packed. The crystal symmetry for $n > 3$ is triclinic, space group $P\bar{1}$ with two formulas per unit cell.

The structure with four different Ti crystallographic sites may also be viewed as containing two types of Ti chains, running parallel to the pseudorutile c axis and truncated, every n Ti sites by the crystallographic shear planes. Accurate determinations of the structure have been made for the three phases by x-ray diffraction methods.[9] In the metallic phase, the four crystallographically independent Ti sites are quite similar, with an average charge of 3.5, as determined by comparing the average Ti–O interatomic distance in each Ti–O octahedron with the Ti^{3+}, Ti^{4+}, and O^{2-} ionic radii. Below 130 K the charges are found to be localized into alternate chains of 3^+ sites

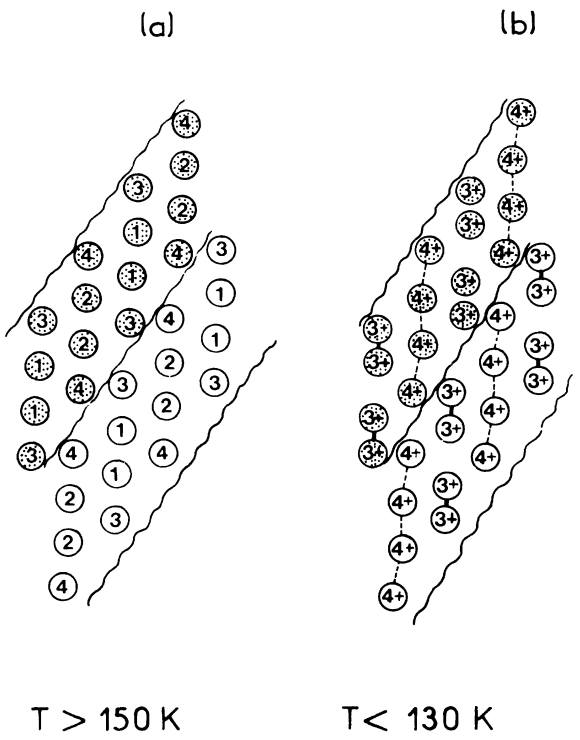

FIG. 1. Crystal structure showing only the Ti chains parallel to the pseudorutile c axis and truncated every four Ti by a crystallographic shear plane: (a) structure in the metallic phase, and (b) structure of the low-temperature phase.

paired to form nonmagnetic metal-metal bonds (Fig. 1). These Ti^{3+}-Ti^{3+} pairs may also be called dimers. In the intermediate phase, no evidence was found for charge localization nor for metallic-bond formation, but anomalously large thermal factors were observed.

The semiconducting properties of the low-temperature phase have to be related with the charge localization shown by the x-ray studies, while the metallic properties of the metallic phase suggest a complete delocalization of the 3*d* electrons. However, the nature of the intermediate phase causes some problems. While the x-ray diffraction data show no charge localization in this phase, the magnetic data show no anomaly at the low-temperature transition; this indicates that the Ti^{3+} pairs still exist in the intermediate phase. A possible model for this phase is therefore a disordered bond model, which would reconcile the crystallographic and magnetic data. This assumption is supported by the anomalously large thermal factors observed on x-ray data in the intermediate phase—the properties and stability of such a disordered phase have been recently discussed by P. W. Anderson, in terms of a "classical liquid of pair bonds."[10] Such a model has also been proposed for the M_3 phase of $V_{1-x}Cr_xO_2$.[11] But NMR and cystallographic data showed that it was not appropriate to this case.[12]

In this paper, we report specific-heat data obtained on Ti_4O_7 single crystals; the enthalpies and entropies of the transitions, previously unknown, give valuable information for the understanding of the nature of the transition. On the basis of these data, we are able to propose a detailed model of disordered bonds for the intermediate phase and show that the low-temperature transition is an order-disorder transition of the Ti^{3+} and Ti^{4+} chains at the unit-cell level.[13]

We also report electron-paramagnetic-resonance (EPR) data for the low-temperature phase, up to the 140-K transition. EPR is one of the ways to investigate microscopic properties and can therefore shed some light on the nature of the low-temperature and intermediate semiconducting phases and on the mechanism of the transition. We have therefore studied a Ti^{3+} center, owing to a deviation from perfect stoichiometry. We show that the line intensity and relaxation are very sensitive to the phase transition. These data establish the dynamic nature of the disorder of the intermediate phase—this is clear experimental evidence of the possibility of studying metal-insulator transitions by EPR.

In Sec. II, we describe the experimental procedure, the crystal growth method, the measurements, and the crystal characterization techniques.

The specific-heat data and their interpretation are presented in Sec. III, and the EPR spectra and their analysis in Sec. IV. In Sec. V, a detailed discussion of the origin of the transitions and of the nature of all three phases is given.

II. EXPERIMENTAL PROCEDURE

The single crystals used in this investigation were grown by chemical transport reaction.[14] The starting material was Ti_3O_5 powder prepared from pure commercial TiO_2 by a hydrogen reduction process. The transport agent was $TeCl_4$. Powder and single-crystal x-ray diffraction showed that the final products were single-phase Ti_4O_7 crystals. These are platelets of dimensions $4\times0.4\times0.1$ mm^3, and are found to be normally twinned. A detailed description of the twin is given elsewhere.[15] The impurity content, as obtained by γ-ray activation analysis,[16] is of the order of several hundreds ppm, with 20–400 ppm of Te, 20–200 ppm of Cl, 20–30 ppm of Cr, and 1–4 ppm of Sc.

The crystals were characterized by electrical resistivity between 80 and 300 K and magnetic susceptibility measurements between 4.2 and 300 K, with a vibrating sample magnetometer in a magnetic field of 10 kG. Typical data are shown in Fig. 2. The susceptibility data show a transi-

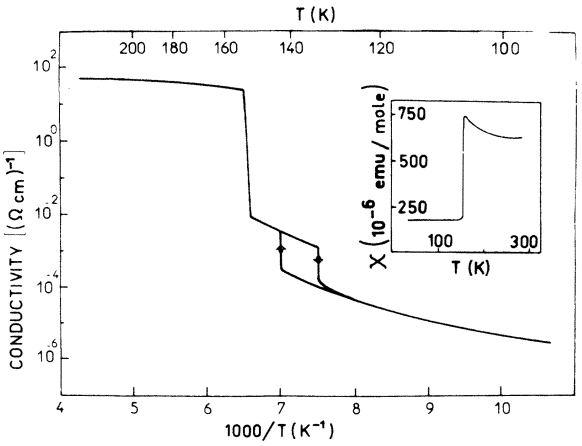

FIG. 2. Conductivity of Ti_4O_7 single crystals—measurements are made along the [0 3 1] pseudorutile direction. Inset shows the magnetic susceptibility vs temperature.

tion at about 150 K without measurable hysteresis. These results are similar to those given in Ref. 6, obtained on crystals grown by flux method elsewhere.[5] The resistivity data show a low-temperature transition with a hysteresis effect of several degrees and a high-temperature transition without hysteresis. Our results are slightly different from those given in Ref. 5. At all temperatures our crystals show a lower conductivity. These discrepancies might be due to the difference in nature of the impurities in the two kinds of samples.

The heat capacity at constant pressure has been measured in the temperature range of 100 to 400 K for several crystals, with a Perkin-Elmer DSC2 differential scanning calorimeter with an accuracy of 2%. This apparatus allows measurements on samples weighing less than 10 mg and is therefore very useful for small single crystals. Measurements have also been performed on larger powder samples at lower temperatures between 10 and 100 K with a differential calorimeter.[17]

EPR spectra were recorded on a CSF-Thomson spectrometer, with a microwave frequency of 9 GHz, over a temperature range from 10 to 140 K (the highest temperature where the spectrum could be resolved).

III. SPECIFIC-HEAT MEASUREMENTS AND ANALYSIS

The heat capacity at constant pressure, C_p is plotted versus temperature in Fig. 3. Two peaks characteristic of first-order transitions clearly appear. The high-temperature peak is centered at 154 K and is 3-K wide; the low temperature peak is about 10-K wide and is centered at 142 K for increasing temperatures and at 130 K for decreasing temperatures. The enthalpies of the transitions are found to be 95 ± 5 and 468 ± 5 cal/mole for the 140- and 150-K transitions respectively. The corresponding entropy changes are 0.70 ± 0.05 and 3.04 ± 0.05 cal/mole K.[13]

A. Low-temperature data

In order to fit the data with the Debye theory, the $C_p - C_v$ correction has been calculated at room temperature with the volume thermal expansion coefficient ($\alpha = 2.9 \times 10^{-5}$ K^{-1}) and the molar volume ($V \simeq 70$ cm^3) deduced from x-ray data for Ti_4O_7,[7] and the tabulated compressibility of TiO_2 ($\beta = 0.57 \times 10^{-6}$ atm^{-1}). The value thus obtained for $C_p - C_v = T\alpha^2 V/\beta$, is found to be 0.7 cal/mole and of the same order of magnitude as the experimental errors on C_p. At low temperature, this correction should be even smaller and therefore negligible. Figure 4 shows the curve of C_p/T vs T^2 obtained from the low-temperature measurements on powder samples. Below 10 K, the Debye law is not obeyed. Between 10 and 40 K, C_p follows a T^3 law corresponding to a Debye temperature of 493 ± 10 K. Above 40 K, the results deviate from the Debye theory and the Debye temperature (as deduced from tabulated values) increases with temperature (Fig. 4, insert).

The departure from the T^3 law below 10 K might be due to some impurities. The Debye temperature of 493 K obtained between 10 and 40 K is smaller than the values of 674 and 760 K obtained for[18] Ti_2O_3 and[19] TiO_2, respectively. The same result has been obtained for V_4O_7 compared to VO_2 and V_2O_3,[20] and might be characteristic of the crystal structure of the Magneli phases. The deviation from the Debye theory above 40 K in-

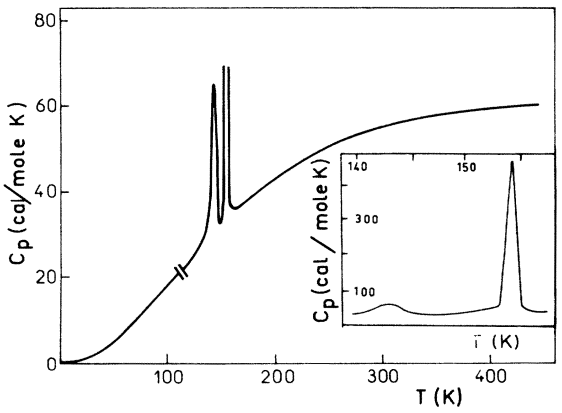

FIG. 3. Molar heat capacity C_p of Ti_4O_7. Measurements are made at low temperature on a powder sample with a weight of 2 g and above 110 K on single crystals with a weight of 25×10^{-3}g. Insert shows the molar heat capacity of single crystals in the temperature range of the transitions with a larger horizontal scale and a smaller vertical one than the main figure. Measurements are performed with increasing temperatures.

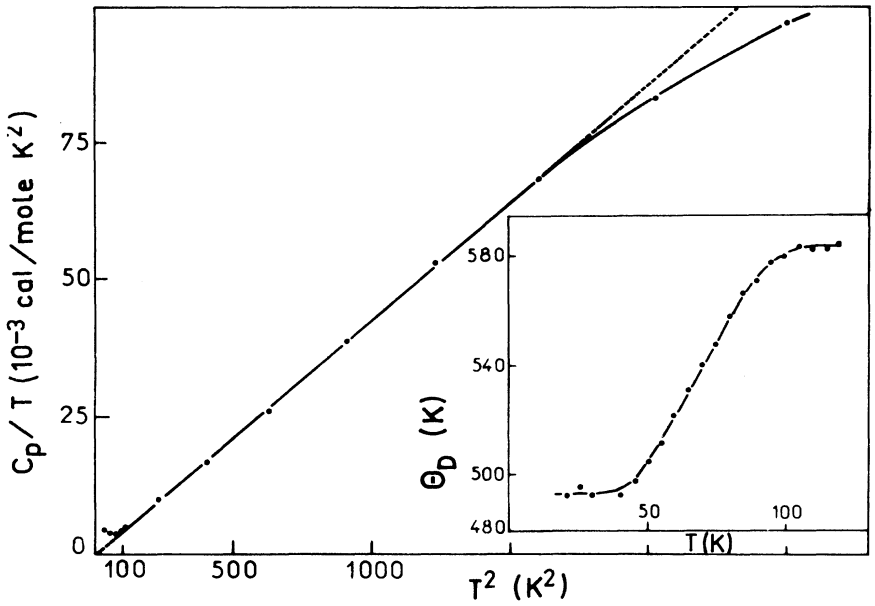

FIG. 4. C_p/T vs T^2 for $T < 50$ K. Corresponding Debye temperature is 493 ± 10 K. Insert shows the Debye temperature θ vs T and the strong deviation from the Debye theory above 40 K.

dicates that the phonon frequency spectrum $g(\omega)$ does not follow the Debye quadratic law even for rather small ω.

B. 140-K transition

As stated in Sec. I, the molar entropy change ΔS at the low-temperature transition may be interpreted in terms of a disordering of the Ti^{3+} bonds. As a first approximation, ΔS may be written as $\Delta S = \frac{1}{2} R \ln W$, where W is the number of configurations per unit cell in the disordered phase. The measured entropy change of 0.70 cal/mole approximately therefore corresponds to two configurations per primitive cell, i.e., for two Ti_4O_7 molecules. This indicates that the disorder of the Ti^{3+} bonds is somewhat limited and suggests a model of disordered Ti^{3+} and Ti^{4+} chains (these chains being four atoms long). The most likely type of disorder, which takes into account the chain structure of Ti_4O_7, is shown in Fig. 5. The crystal structure is such that at all temperatures there are two types of Ti chains: the *a* chains corresponding to the crystallographic sites 3-1-1-3 and the *b* chains to the sites 4-2-2-4. In the low-temperature ordered phase, the Ti^{3+} dimers are always on the *a* chains and the Ti^{4+} ions on the *b* chains. In the disordered intermediate phase, the two Ti^{3+} dimers would be located either on an *a* chain or on a *b* one, and similarly for the Ti^{4+} ions. In order for this model to be crystal chemically reasonable, one has to add the following restriction: no more than two consecutive chains could be occupied by the same type of ions. The presence of more than two consecutive chains occupied by the same ions would lead to a very large local extra energy. Such a configuration would not be probable. One may note that the crystallographic blocks separated by the shear planes are not correlated and that this model corresponds to a short-range order along the pseudorutile *c* axis involving four atoms only. This type of disorder relative to ionic charges and

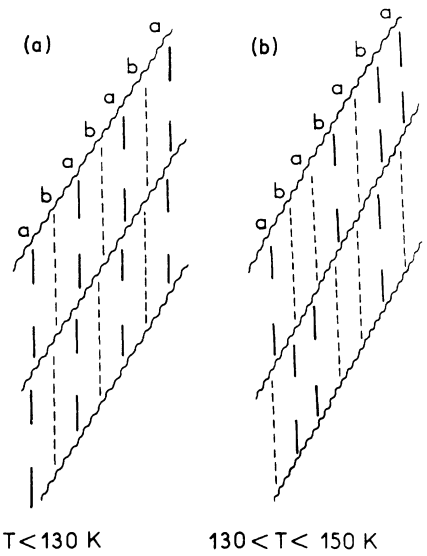

FIG. 5. Proposed model for the disorder of the Ti chains; (a) structure of the low-temperature phase—Same as Fig. 1(b). (b) Structure with disordered Ti^{3+}-Ti^{3+} pairs for the intermediate phase. The *a* (3 – 1 – 1 – 3) chains contain the Ti(1) and Ti(3) sites, while the *b* (4 – 2 – 2 – 4) chains contain the Ti(2) and Ti(4) sites [see Fig. 1(a)].

slight atomic displacements cannot be visualized by classical x-ray methods. Especially, one does not expect any superlattice lines in the x-ray pattern below 130 K, as the form factors of the Ti^{3+} and Ti^{4+} ions are approximately the same.

The previous argument of two configurations per unit cell is crude, as Ti_4O_7 is not a molecular crystal. A correct calculation of the entropy of the system needs more sophisticated mathematics. The same kind of problem has been solved for the Ising model[21] and for chain molecules[22] by a matricial technique. It is clear from Fig. 5 that there are four possible configurations for two successive chains. Let us call $Ti^{3+}(c)$-$Ti^{4+}(c)$, the configuration of the unit cell stable in the low-temperature phase, $Ti^{3+}(c)$ meaning a Ti^{3+} chain and $Ti^{4+}(c)$, a Ti^{4+} one. The four configurations in the intermediate phase are:

$$Ti^{3+}(c)\text{-}Ti^{4+}(c),\ \alpha_1;\quad Ti^{4+}(c)\text{-}Ti^{3+}(c),\ \alpha_2;$$

$$Ti^{3+}(c)\text{-}Ti^{3+}(c),\ \alpha_3;\quad Ti^{4+}(c)\text{-}Ti^{4+}(c),\ \alpha_4.$$

Let us define the configurational matrix correlating the configuration of a pair of chains to that of the next pair of chains inside a block:

$$\underline{M}=\begin{pmatrix} U_{\alpha_1\alpha_1} & U_{\alpha_1\alpha_2} & \cdots & \cdots \\ U_{\alpha_2\alpha_1} & \cdots & \cdots & \cdots \\ U_{\alpha_3\alpha_1} & \cdots & \cdots & \cdots \\ U_{\alpha_4\alpha_1} & \cdots & \cdots & \cdots \end{pmatrix},$$

where $U_{\alpha_i\alpha_j}$ is the statistical weight of the configuration $(\alpha_i\alpha_j)$ for two pairs of chains. The notion of statistical weight for a given configuration is based on physical grounds and is related to the energy $E_{\alpha_i\alpha_j}$ of this configuration by

$$U_{\alpha_i\alpha_j}=\exp[-(E_{\alpha_i\alpha_j}/kT)].$$

One can then show[22] that the number of configurations of N pairs of chains ($2N$ Ti_4O_7 molecules) is

$$W=\lambda^N,$$

where λ is the largest eigenvalue of the $\underline{M}$ matrix. The molar entropy change at the transition is given by

$$\Delta S=\tfrac{1}{2}R\ln\lambda .$$

The values of $U_{\alpha_i\alpha_j}$ are determined by the physical properties of the system. A statistical weight of one is chosen for the configuration stable at low temperature: $U_{\alpha_1\alpha_1}=U_{\alpha_2\alpha_2}=1$, which corresponds to $E_{\alpha_1\alpha_1}=E_{\alpha_2\alpha_2}=0$. From the restriction that no more than two consecutive chains are occupied by ions of similar charge, it follows that $U_{\alpha_2\alpha_3}=0$. Let us define $U_{\alpha_2\alpha_1}=p\leq 1$ and $U_{\alpha_4\alpha_3}=q\leq 1$.

As a first approximation, one can assume that $q\sim p^2$ since the energies of the configurations should be approximately $E_{\alpha_4\alpha_3}\sim 2E_{\alpha_2\alpha_1}$. We therefore obtain for the configurational matrix:

$$\underline{M}=\begin{pmatrix} 1 & p & p & 0 \\ p & 1 & 0 & p \\ 0 & p & 0 & p^2 \\ p & 0 & p^2 & 0 \end{pmatrix}.$$

In the case of $p\lesssim 1$, the largest eigenvalues of this matrix are

$$\lambda=(3+\tfrac{1}{2}\sqrt{5})-(1-p)(15+\tfrac{3}{10}\sqrt{5}) .$$

As λ is always smaller than $(3+\frac{1}{2}\sqrt{5})=2.62$, this gives

$$S<0.96\ \text{cal/mole} .$$

The experimental value of 0.70 cal/mole corresponds to $p\sim 0.70$. This gives an extra energy $E_{\alpha_1\alpha_2}$ of about 3 meV for the configurations such as $\alpha_1\alpha_2$ compared to the configuration $\alpha_1\alpha_1$ stable below 130 K. The low-temperature transition takes place at a temperature T such that $E_{\alpha_1\alpha_2}\sim 0.3\,kT$.

C. 150-K transitions

The high-temperature transition has to be attributed to a delocalization of the $3d$ electrons. The entropy of this transition includes an electronic term and possibly a lattice term. One can estimate the electronic term from the susceptibility data (Fig. 2). In both low-temperature and intermediate phases, the temperature-independent susceptibility is due to a Van Vleck orbital mechanism. The steep increase of the susceptibility at 150 K is due to a Pauli term. If one assumes that the Van Vleck term is negligible in the metallic phase (this will be discussed in Sec. VI), the Pauli susceptibility is of the order of 600 to 750 $\times 10^{-6}$ emu/mole. This value corresponds to an effective mass m^* of 15 to 18m, m being the free electron mass, and to a density of states at the Fermi level of 10–12 eV^{-1} per $3d$ electron.

The susceptibility appears to be quite enhanced, as in similar materials such as[23] VO_2 and other vanadium oxides.[20] Such an enhancement can be due to two different mechanisms. The first one is related to the Brinkman–Rice[24] model of a highly correlated electron gas. In this model, the enhancement factor is the same for the coefficient of the electronic specific heat as for the Pauli susceptibility. This leads to a γ value of approximately 0.01 cal/mole K^2 and an electronic entropy change of 1.50 cal/mole K. As the total entropy change is 3.04 cal/mole K, the electronic contribution would be of the same order of magnitude as the lattice contribution.

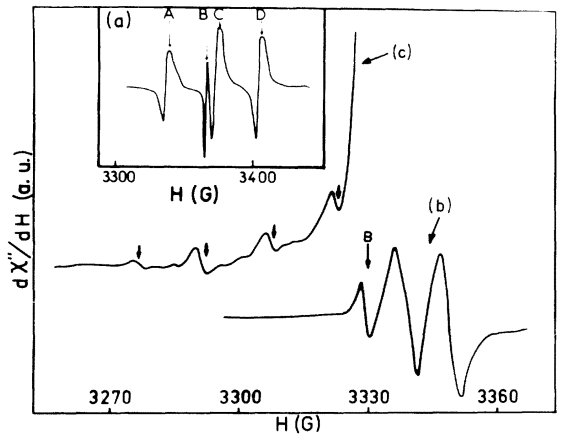

FIG. 6. EPR spectra of untwinned Ti_4O_7 single crystals at 80 K. (a) Typical spectra showing the four lines *A*, *B*, *C*, and *D*. (b) Spectrum recorded for a different field orientation. (c) Same as (b) recorded with a higher sensitivity showing the Ti hyperfine structure of the *B* line.

In the second mechanism, the Pauli susceptibility is exchange enhanced.[25] One does not expect in this case any enhancement of the γ coefficient. This leads to a result where the entropy of the transition would be entirely due to the lattice, which seems unreasonable in the case of Ti_4O_7.

Therefore, we conclude that the electronic and lattice contributions to the entropy of the 150-K transition are approximately the same. The electron-phonon coupling should play an important part in the mechanism of this transition.

IV. ELECTRON-PARAMAGNETIC-RESONANCE SPECTRA AND ANALYSIS

One does not expect any intrinsic EPR signal in the semiconducting phases of a perfectly stoichiometric Ti_4O_7 crystal, as the 3*d* electrons are paired in nonmagnetic metal-metal bonds. However, any dilute magnetic center can act as an EPR probe and give precious information on the nature of the low-temperature phase and on the approach to the transition. EPR data have already been reported on Ti_4O_7 powders.[26] But single-crystal data are necessary to identify the magnetic centers and to relate their relaxation behavior to the Ti_4O_7 host properties.

A. Experimental data

We performed EPR measurements on untwinned Ti_4O_7 crystals in order to obtain meaningful data.[27] As the untwinned crystals are in any case very small (1 mm^3 or less) the measurements had to be very accurate. At 10 K, as-grown Ti_4O_7 crystals show about ten unidentified lines, most of which are not detected at 80 K owing to their short relaxation times. The four principal lines of a typical spectrum obtained at 80 K are shown in Fig. 6(a). The so-called *B* line has the smallest linewidth and can be followed up to the low-temperature transition; hence it serves as an ideal EPR probe. The other lines cannot be detected at temperatures higher than approximately 100 K and will not be discussed any further.

The spectrum is shown in Fig. 6(b) for a different field orientation. In this case a hyperfine structure with eight lines is detected for the *B* line and is shown on Fig. 6(c) at 80 K. The values and axes of the *g* and hyperfine tensors, measured at 80 K, are reported in Table I.

The intensity of this line has been measured by comparison with a known sample of P-doped Si and is plotted versus temperature in Fig. 7. The same figure shows $1/\chi_B$ vs T, which indicates that below 130 K a Curie-Weiss law is well-obeyed with a negative Curie temperature of the order of 10 K. The spin concentration is found to be of the order of 4×10^{19} centers/mole. Above 130 K, the intensity of the line decreases abruptly and is not

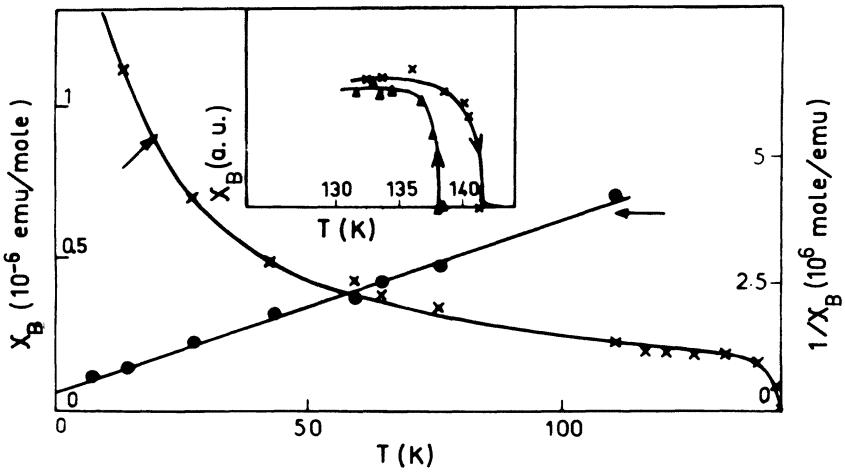

FIG. 7. Integrated intensity χ_B of the *B* line vs temperature (×). Reciprocal intensity $1/\chi_B$ vs temperature showing a Curie-Weiss behavior (●). Insert shows the hysteresis of $\chi_B(T)$ in the transition region.

TABLE I. Principal values of the g tensor and of the hyperfine A tensor for the EPR B line observed at 80 K on Ti_4O_7 single crystals. θ and ϕ are the spherical coordinates of the tensor axes referred to the pseudorutile axes.

g	θ	ϕ	A (cm^{-1})	θ'	ϕ'
1.932	126°	47°	36.6×10^{-4}	78°	49°
1.952	75°	−57°	17.0×10^{-4}	104°	−44°
1.965	41°	50°	6.3×10^{-4}	20°	−1°

detectable anymore above 140 K. The vanishing of the line takes place at the same temperature as the semiconducting-semiconducting transition. This result is significantly different from that obtained on powder samples.[26] The hysteresis of the line intensity, shown in the inset of Fig. 7, corresponds approximately to that obtained by electrical resistivity and specific-heat measurements. Figure 8 shows the dependence with temperature of the peak-to-peak linewidth, ΔH, which is always small (1 to 4 G). Below 60 K, it decreases with increasing temperature. Above 80 K, ΔH increases rapidly, showing two anomalies at 130 and 140 K where the line vanishes. The g tensor of this line remains unchanged between 10 and 135 K and the line shape is approximately Lorentzian in the same temperature range. The hyperfine structure is resolved from 10 to approximately 130 K.

B. Analysis of the center

The observed structure of the B line is characteristic of Ti nuclei.[28,29] The two isotopes ^{47}Ti and ^{49}Ti, with a natural abundance of 7.5 and 5.51 % have nuclear spins $\frac{5}{2}$ and $\frac{7}{2}$, respectively, and approximately the same nuclear frequency. The total intensity of the eight observed hyperfine lines compared to the main peak corresponds to the abundance of the two isotopes (~13%).

Since the g value is slightly smaller than two, and since the spectrum does not show any fine structure, the line may be ascribed to a Ti^{3+} ($3d^1$) center. The g-tensor axes are not related simply to any crystallographic axis, because of the low triclinic symmetry. Also, they do not give any information on the orbital state. However, the hyperfine tensor axes are found roughly parallel to the pseudorutile [1 1 0], [1 $\bar{1}$ 0], and [0 0 1] directions.

This result indicates that the Ti^{3+} center is located on a normal Ti site. As a first approximation, we may assume that the crystal field is orthorhombic, with axes parallel to the pseudorutile [1 1 0], [1 $\bar{1}$ 0], and [0 0 1] directions. As the crystal-field splittings are much larger than the spin-orbit coupling, the energy levels are as shown on Fig. 9. As an EPR signal is observed, the lowest state is mainly an x^2-y^2 orbital state, with x and y axes parallel to the c and [1 1 0] pseudorutile axes, respectively.[30]

From the observed deviation from two for the g tensor, it is possible to estimate the splittings Δ_1 and Δ_2 between the ground state and the zy and zx excited states. If $\Delta g = 2-g$, one expects $\Delta g/g \sim \lambda/\Delta$, where λ is the spin-orbit coupling constant. With the Ti^{3+} free-ion value of $\lambda = 154$ cm^{-1},[31] one obtains Δ_1 and Δ_2 of the order of 3000 cm^{-1} (~0.4 eV). Since there might be a large reduction of λ due to covalent bonding, these values are upper

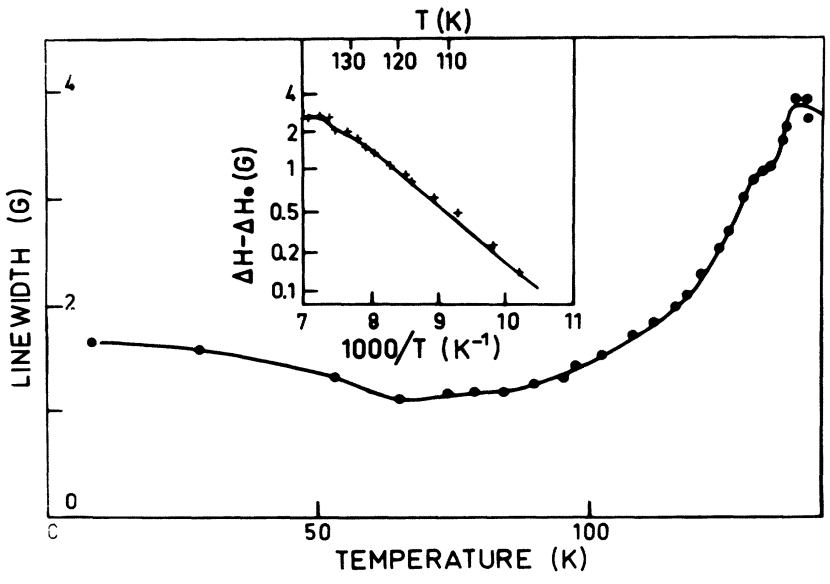

FIG. 8. Width ΔH of the B line vs temperature. Insert shows the temperature-dependent part of the linewidth vs reciprocal temperature. ΔH_0 is a temperature-independent contribution to ΔH, determined in the temperature range of 60 to 80 K ($\Delta H_0 = 0.27$ G).

limits of Δ_1 and Δ_2. However, they are indicative of a strong orthorhombic crystal-field splitting.

The hyperfine tensor values may be compared with those expected in a crystal of tetragonal symmetry.[32] If $\lambda/\Delta \ll 1$, one expects

$$A_{\parallel} \sim a + (\tfrac{4}{7})\, P, \quad A_{\perp} \sim a - (\tfrac{2}{7})\, P.$$

$A_{\parallel}$ and $A_{\perp}$ are the hyperfine values parallel and perpendicular to the crystal axis, respectively. a is the isotropic contact hyperfine contribution and P the anisotropic part

$$P = 2\gamma \mu_B \mu_N \langle r^{-3} \rangle,$$

γ is the nuclear gyromagnetic ratio; μ_B and μ_N are, respectively, the Bohr and nuclear magnetons; r is the distance electron nucleus, and $\langle r^{-3} \rangle$ an average value taking into account the radial distribution function of the electron.

In our case, if one takes for $A_{\parallel}$ the principal value corresponding to the hyperfine tensor axis roughly parallel to the c pseudorutile axis and for $A_{\perp}$ the average between the two other values, one obtains

$$a \sim 19.9 \times 10^{-4}\ \text{cm}^{-1}; \quad P \sim -23.9 \times 10^{-4}\ \text{cm}^{-1},$$

$$\langle r^{-3} \rangle \sim 2.39\ \text{a.u.}$$

These values are similar to those found in MgO or CaO.[29] The $\langle r^{-3} \rangle$ calculated value for a Ti^{3+} free ion is 2.55 a.u., of the same order of magnitude as our experimental value.

The presence of unpaired Ti^{3+} ions in Ti_4O_7 may be the result of several mechanisms. They could be due to the incorporation of impurities such as trivalent nonmagnetic impurities on Ti sites breaking Ti^{3+} pairs, or to stoichiometry defects. As we observe the same center in crystals grown by different methods (flux method or vapor transport with HCl instead of Te Cl_4 as transport agent), we rule out the first explanation. It has not been possible to measure the stoichiometry of the samples, because of their small size. The EPR spectrum could be due to oxygen vacancies, as suggested by Houlihan *et al.*[26] or to Ti vacancies. We feel that oxygen vacancies are unlikely as the oxygen lattice in the Magneli phase should be rather stable. Moreover, we observed that V doping decreases sharply the intensity of the Ti line, indicating that V compensates a stoichiometry defect.

A titanium vacancy, depending on its location either on a Ti^{3+} or Ti^{4+} site, converts three or four neighboring Ti^{3+} ions into Ti^{4+} in order to keep charge neutrality. In the process, it may leave a cluster of unpaired Ti^{3+} ions, located on Ti_3 or Ti_1 sites. Such clusters or Ti^{3+} centers are responsible for a non-negligible exchange interaction below 40 K, as shown by the Curie-Weiss behavior, although the total B-center spin concentration is relatively low.

C. Temperature behavior

The linewidth shows a peculiar temperature dependence. The value measured at the lowest temperature is the intrinsic linewidth due to the dipole-dipole interaction. Although the observed spin concentration should correspond to a dipolar linewidth of 10^{-2} G, the presence of clusters (as stated above) leads to a much larger dipolar linewidth (~ 2 G). It is suggested that the decrease of ΔH vs temperature is due to a motional narrowing related to a hopping process. In such a process, the linewidth (in frequency units) is $\Delta\omega = \omega_{dip}^2/\omega_{mot}$,[33] where ω_{dip} is the frequency related to the dipolar interaction and ω_{mot} the rate of motion of the hopping electron. We deduce a correlation time for the motion which decreases with increasing temperature, down to 2×10^{-8} sec at 60 K. As the characteristic time for the hyperfine interaction is of the order of 5×10^{-9} sec, the hyperfine structure is not washed out by this process. Such a mechanism assumes that the electron hops between equivalent crystallographic sites; this hopping process is possible because of the presence of B-center clusters.

Between 60 and 90 K, the linewidth is approximately temperature independent; its value ΔH_0 is probably the smallest possible one, owing to crystal-field inhomogeneities or other imperfections.

The increase of ΔH above 90 K suggests that the dominant mechanism is then due to spin-lattice relaxation. The temperature-dependent part of the linewidth $\delta H = \Delta H - \Delta H_0$, has to be assigned to the longitudinal relaxation time τ_1. One could interpret δH by a two-phonon Raman process.[34] Such a process induces a T^9 temperature dependence for Kramers's ions such as Ti^{3+}. In our case, a power law of $T^{7.7}$ can be fitted; however, the preexponent coefficient is found to be 10^{-17} G, which is much smaller than the usual values ($\sim 10^{-5}$ G) for most materials.[34] We would rather suggest that the relaxation is due to an excited state, therefore to a resonant Orbach process. In the inset of Fig. 8 ($\delta H = \Delta H - \Delta H_0$) is plotted vs $1/T$. Good

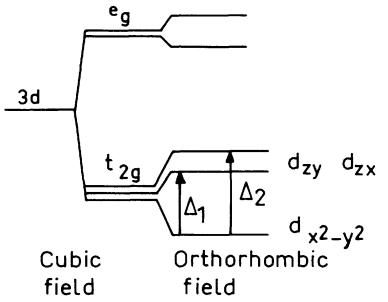

FIG. 9. Crystal-field splittings of a $3d^1$ level.

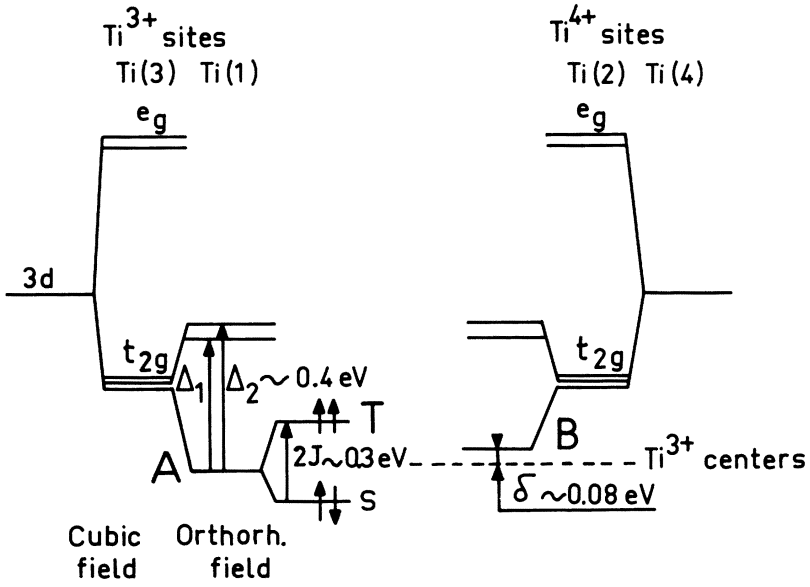

FIG. 10. Atomic and molecular levels scheme for the Ti^{3+} chains (left and for the Ti^{4+} chains (right).

agreement is found with the law: $\delta H \sim e^{-\delta/kT}$ with $\delta \sim 0.08$ eV ~ 930 K. Obviously, a two-phonon Orbach process cannot be invoked as δ is much larger than kT and even larger than the Debye energy ($\Theta_D \sim 500$ K). Therefore, we conclude that only a multiphonon Orbach process can account for our results. A four-phonon mechanism has already been proposed for the relaxation of V^{4+} in[35] TiO_2 and has been theoretically discussed in Ref. 36. It is clear that the excited state, situated 0.08-eV above the Ti^{3+} level, cannot be attributed to the Ti^{3+} excited states, as the crystal-field splittings have been previously shown to be of the order of 0.4 eV. If the Ti^{3+} center is located on a Ti^{3+} site [Ti(3) or Ti(1)], then the empty level corresponding to the Ti^{4+} sites [Ti(4) or Ti(2)] should lie a few hundreths of an eV above the Ti^{3+} level. We propose that the Orbach process takes place through these empty Ti^{4+} levels.

The softening of the temperature dependence of the relaxation near 130 K indicates a decrease of the splitting between these two levels. Such a decrease is expected at the low-temperature transition, as in the disordered intermediate phase, the Ti^{3+} ions are located either on the Ti^{3+} or on the Ti^{4+} sites of the low-temperature structure. The scheme of the levels is discussed in more detail in Sec. VI.

As the 140-K transition is approached, the intensity of the EPR signal decreases rapidly (see Fig. 7). It is obvious that this is not due to a conductivity effect as the skin depth in the intermediate phase is about 5 mm and the crystals are not more than 0.1-mm thick. But at the low-temperature transition (according to the model given in Sec. IV) the Ti^{3+} pairs become disordered. The vanishing of the EPR signal indicates that the disorder of the intermediate phase is dynamic. When the Ti^{3+} pairs get mobile, the electrons of the broken bonds also hop through the crystal. Two different mechanisms may explain the vanishing of the EPR signal. Either, the lifetime of the unpaired electrons on a given site becomes shorter than 10^{-10} sec, or in the hopping process, no unpaired electrons are left through the crystal. The first mechanism seems more likely. Therefore, this result would indicate that the lifetime of the electrons on a given site becomes less than 10^{-10} sec in the intermediate phase.

The rapid decrease of the B-line intensity through a few degrees, correlated with the width of the specific-heat peak seems due to nucleation of the domains of the intermediate phase. Since the B-line intensity decreases sharply above 135 K, the behavior of the linewidth just at the transition may be not significant and will not be discussed any further.

V. DISCUSSION

A. Low-temperature phase

The ordering of the Ti^{3+} dimers on one type of chain in the low-temperature phase leads to the level scheme shown in Fig. 10. As a first approximation, we do not take into account any possible broadening of the atomic or molecular levels into bands. We separate the Ti sites into two types, the Ti(1) and Ti(3) sites occupied by the Ti^{3+} ions, and the Ti(2) and Ti(4) sites occupied by the Ti^{4+} ions. We assume that the crystal-field splittings are approximately the same for the Ti(1) and Ti(3) sites and for the Ti(2) and Ti(4) sites, respective-

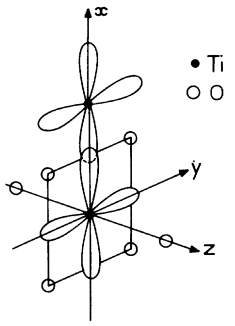

FIG. 11. Pair formation by orbital overlap along the pseudorutile c axis.

ly. Obviously this is not completely true as the oxygen octahedra surrounding the Ti(1) and Ti(3) sites, for example, are slightly different. The fivefold orbital d state is split into a lowest triplet t_{2g} and a highest doublet e_g by a cubic octahedral crystal field. The orthorhombic component of the crystal field then splits the t_{2g} triplet into three orbital singlets. The lowest orbital singlet should then correspond approximately to a $d_{x^2-y^2}$ state. This level should be slightly lower for the Ti^{3+} sites (A level) than for the Ti^{4+} (B level), as shown in Fig. 10. On the Ti^{3+} chains, as the Ti^{3+} pairs are formed, the $d_{x^2-y^2}$ orbital state gives rise to a lowest bonding spin singlet state S and a highest antibonding spin triplet state T. The S and T states correspond to molecular orbitals built with the $d_{x^2-y^2}$ orbitals of two neighboring Ti(1) and Ti(3) sites (see Fig. 11).

We may estimate a value for the splitting $2J$ between these bonding and antibonding states from the temperature behavior of the magnetic susceptibility χ. As χ is temperature independent up to 150 K, there is no direct contribution coming from an increase of the population of the triplet state versus temperature. This indicates that $2J$ is certainly larger than 0.2 eV. Then χ is due only to the Van Vleck matrix elements between the singlet S state and some excited state. It seems then reasonable to assume that this excited state is the triplet state. One may obtain a rough order of magnitude for the $2J$ splitting between S and T, by the formula[37]

$$\chi_{VV} \sim N\mu_B^2/2J ,$$

where N is the number of electrons of the ground state. A value for $2J$ of 0.3 eV is deduced.

In Sec. V we proposed that the Orbach relaxation of the Ti^{3+} B center above 100 K was due to the empty higher levels corresponding to the Ti^{4+} ions. One may assume that the orbital ground state of the unpaired Ti^{3+} is very near to the A level. Then the energy δ obtained from the Orbach process gives ~0.1 eV for the splitting between the A and B levels, which are the ground states of the Ti^{3+} and Ti^{4+} ions in the low-temperature phase.

As the 140-K transition is approached, this splitting should decrease and δ should become zero in the intermediate phase where the Ti^{3+} and Ti^{4+} ions occupy both kinds of sites. This is in agreement with the softening of the relaxation process just below the transition.

The transport of the low-temperature phase might also be related to the empty Ti^{4+} levels. However, the conductivity curve versus temperature (Fig. 2) does not show at low temperature a well-defined activation energy. It was already suggested in Ref. 26 that crystal defects, mainly related to nonstoichiometry are responsible for the transport properties below 120 K. Between 120 and 140 K, the conductivity behavior may be described by an activation energy $E_a \sim 0.16$ eV. Figure 2 shows that an activation energy of the same order of magnitude may be attributed to the intermediate phase. We propose that in this temperature range, the transport properties are intrinsic and related to a hopping process of the $3d$ electrons of the Ti^{3+} sites. The possible mechanism for this hopping will be discussed in Sec. V B. The ordering of the Ti^{3+} ions on one type of chain in the low-temperature phase has some similarity with the classical Verwey model proposed for Fe_3O_4.[38] The properties of such a system have been discussed by Mott.[39] They involve interatomic electronic correlations and should depend on the ratio V_0/B, V_0 being the interaction potential between carriers on nearest-neighbor sites and B the width of a band built on the $3d$ orbitals. However, the presence of the pairs of Ti^{3+} differentiates Ti_4O_7 from Fe_3O_4. In our case, V_0 should be the interaction between dimers located on neighboring Ti chains and B the width of a band built through overlap of the orbitals from one chain to the adjacent one. This rather small overlap should lead to a value for V_0/B larger than one and therefore to the pair crystallization at low temperature.

B. Intermediate phase

As was proposed in Sec. IV, the intermediate phase is a disordered phase as far as the Ti^{3+} dimers are concerned. The low-temperature transition is then an order-disorder transition and is driven by the disorder entropy of these dimers. At 140 K, this disorder entropy takes over the interpair correlation energy.

The Van Vleck magnetic susceptibility of the low-temperature phase was attributed to the matrix elements between the singlet and triplet states of the pairs. As the susceptibility does not show any anomaly at 140 K, we conclude that the short Ti^{3+}-

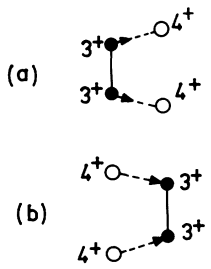

FIG. 12. Bipolaron conductivity process for the intermediate phase. Two electrons of a Ti^{3+} pair simultaneously leave their site towards an adjacent Ti chain (a). Another Ti^{3+} pair is formed on the adjacent chain (b).

Ti^{3+} distance is the same in the disordered phase as in the low-temperature "condensed" phase.

It has been shown in Sec. V that this disorder is dynamic. Our model is then similar to the one proposed by P. W. Anderson[10] for systems with one electron per cation site, involving resonating valence bonds, i.e., two paired electron bonds wandering through the crystal. However, in our case, there is only one electron per two sites and in order to destroy one pair and to create another, both electrons must hop between sites by pairs.

Therefore we rather propose that the intermediate phase should be treated as a gas of two-particle polarons, or *bipolarons*. Such a model has already been proposed by N. F. Mott[40] and recently theoretically discussed by P. W. Anderson[41] for amorphous materials. In this model, owing to strong electron-phonon coupling, the Hubbard interaction between up and down spins on the same bond may be attractive because of the formation of the bond between the two cations. Also, there is no gap for a two-electron excitation and any observed gap is a mobility one.

In the case of Ti_4O_7, one may attribute a half-filled bipolaron band to the intermediate phase. The conduction mechanism is shown in Fig. 12: the two electrons of a Ti^{3+} pair simultaneously leave their sites and form another pair on the adjacent chain which was previously occupied by Ti^{4+} ions. The two electrons therefore diffuse together with a local lattice distortion, just as in the small polaron theory.[42] This process is a bipolaron diffusion. The experimental activation energy of 0.17 eV is then a mobility activation through phonons. At the low-temperature transition, the ordering of the Ti^{3+} pairs corresponds to a gap opening in the bipolaron band, driven by the interpair correlation energy. However, just below the transition this energy gap is rather small and the electrical conductivity may also take place through bipolaron hopping, just as in the intermediate phase. The observed activation energy is then a result of both this energy gap and the activation energy for the bipolaron mobility.

C. Metallic phase

It was shown in Sec. IV that the 150-K transition entropy can be accounted for by an electronic and a lattice contribution of approximately the same magnitude. Also at this transition, the unit-cell parameters and volume undergo an abrupt change.[7] These two facts indicate that this transition is induced by an electron-phonon interaction. The transition by decreasing temperature leads to the polaronic intermediate phase, essentially because there is only one electron per two sites. The distortion of the system is then local and not long range.

The relatively high value of the magnetic susceptibility (750 emu/mole) at 152 K and the large electronic contribution to the high-temperature transition entropy (~ 1.5 cal/mole K) show that the electronic effective mass is enhanced by electronic correlations in a manner similar to that proposed by Brinkman and Rice for other materials.[24] But in the case of Ti_4O_7, only *interatomic* electronic correlations are likely to be important. The intra-atomic correlations should not be effective because of the one electron per two sites.

The rather poor conductivity of the metallic phase is probably due to a lowering of the mobility induced by impurities such as Te and Cl. The material might be intermediate between a pure metal and an Anderson insulator where localization occurs by impurity potential perturbation.[43]

VI. CONCLUSIONS

The most interesting feature of the titanium oxide Ti_4O_7 lies in the nature of the semiconducting intermediate phase. It is shown in this paper that all the presently known data can be accounted for by a dynamical disorder of Ti^{3+} pairs in this phase. The detailed model of disorder along Ti chains is in agreement with the measured value of the entropy of the transition. Such a model might be corroborated only by x-ray diffuse scattering. This phase is also believed to be an illustration of the bipolaronic state proposed by several authors. The possibility of growing larger crystals and of stabilizing this disordered phase in a larger temperature range and down to lower temperatures would allow an improved study of this phase by other methods, such as optical and inelastic neutron scattering measurements.

ACKNOWLEDGMENTS

The authors wish to thank J. Mercier for his main contribution to the crystal growing, and all the technical staff of the Groupe des Transitions

de Phase without whom this work could not have been performed. They acknowledge helpful discussions with Y. Merle d'Aubigné, K. A. Muller, and D. K. Ray for the EPR results and with F. de Bergevin for the entropy calculation. They are especially grateful to Sir Nevill Mott for his great interest in this work and for illuminating discussions.

---

*Research supported in part by an "Action Thématique Programmée Matériaux" from Center National de la Recherche Scientifique.

†This work is part of a thesis submitted by S. Lakkis to the Université Scientifique at Médicale de Grenoble, in partial fulfillment of the requirement for the degree of Docteur d'Etat.

[1]N. F. Mott, *Metal-Insulator Transitions* (Taylor and Francis, London, 1974).
[2]J. B. Goodenough, Prog. Solid State Chem. 5, 145 (1972).
[3]B. K. Chakraverty, J. Solid State Chem. 12, 376 (1975).
[4]S. Anderson and L. Jahnberg, Ark. Kemi 21, 413 (1963).
[5]R. F. Bartholemew and D. F. Frankl. Phys. Rev. 187, 828 (1969).
[6]W. J. Danley and L. N. Mulay, J. Appl. Phys. 41, 877 (1970).
[7]M. Marezio, P. D. Dernier, D. B. McWhan, and J. P. Remeika, Mater. Res. Bull. 5, 1015 (1970).
[8]M. Marezio and P. D. Dernier, J. Solid State Chem. 3, 340 (1971).
[9]M. Marezio, D. B. McWhan, P. D. Dernier, and J. P. Remeika, J. Solid State Chem. 6, 213 (1973).
[10]P. W. Anderson, Mater. Res. Bull. 8, 153 (1973).
[11]T. M. Rice, AIP Conf. Proc. 10, 1406 (1972).
[12]J. P. Pouget, H. Launois, T. M. Rice, P. Dernier, A. Gossard, G. Villeneuve, and P. Hagenuller, Phys. Rev. B 10, 1801 (1974).
[13]C. Schlenker, S. Lakkis, J. M. D. Coey, and M. Marezio, Phys. Rev. Lett. 32, 1318 (1974); C. Schlenker, S. Lakkis, M. Marezio, and R. Buder, Franco-British Centenary Conference, Jersey, 1974 (unpublished).
[14]J. Mercier and S. Lakkis, J. Cryst. Growth 20, 195 (1973).
[15]J. L. Hodeau, M. Marezio, C. Schlenker, R. Buder, and S. Lakkis (unpublished).
[16]The γ-ray activation analysis has been performed at Laboratoire Central d'Analyse et de Contrôle, Centre d'Etudes Nucléaires de Grenoble.
[17]R. Lagnier, Report No. C. E. A.-R-4419 (1973) (unpublished). These measurements have been performed in the Service de Basses Températures, Centre d'Etudes Nucléaires de Grenoble.
[18]M. E. Sjöstrand and P. H. Keesom, Phys. Rev. B 7, 3558 (1973).
[19]P. H. Keesom and N. Pearlman, Phys. Rev. 112, 800 (1958).
[20]D. B. McWhan, J. P. Remeika, J. P. Maita, H. Okinaga, K. Kosuge, and S. Kachi, Phys. Rev. B 7, 326 (1973). The Debye temperatures calculated from the coefficient of the T^3 law given in this paper are 410, 496, and 591 K for V_4O_7, V_2O_3, and VO_2, respectively.
[21]G. F. Newell and E. W. Montroll, Rev. Mod. Phys. 25, 353 (1953).
[22]P. J. Flory, *Statistical Mechanics of Chain Molecules* (Wiley-Interscience, New York, 1969), p. 66.
[23]G. V. Chandrashekhar, H. L. C. Barros, and J. M. Honig, Mater. Res. Bull 8, 369 (1973).
[24]W. F. Brinkman and T. M. Rice, Phys. Rev. B 2, 4302 (1970).
[25]J. R. Schrieffer, J. Appl. Phys. 39, 642 (1968).
[26]J. F. Houlihan and L. N. Mulay, Phys. Status Solidi B 61, 647 (1974); J. F. Houlihan, W. J. Danley, and L. N. Mulay, J. Solid State Chem. 12, 265 (1975).
[27]S. Lakkis, R. Buder, C. Schlenker, and B. K. Chakraverty, Fifth International Symposium on Magnetic Resonance, Bombay, Jan. 1974. (unpublished).
[28]D. F. Schirmer and K. A. Müller, Phys. Rev. B 7, 2986 (1973).
[29]J. J. Davies and J. E. Wertz, J. Magn. Res. 1, 500 (1963).
[30]See for example, J. W. Orton, *Electron Paramagnetic Resonance* (Iliffe, London, 1968), p. 115.
[31]A. Abragam and B. Bleaney, *Electron Paramagnetic Resonance of Transition Ions* (Clarendon, Oxford, 1970), p. 399.
[32]A. Abragam and M. H. L. Price, Proc. R. Soc. A 205, 135 (1953).
[33]P. W. Anderson and P. R. Weiss, Rev. Mod. Phys. 25, 269 (1953).
[34]See Ref. 31, pp. 60 and 541.
[35]V. N. Bogomolov, E. S. Kudinov, S. T. Pavlov, and L. S. Sochava, Fiz. Tverd. Tela. 10, 20 43 (1968) [Sov. Phys. Solid State 10, 1604 (1969)].
[36]S. S. Bashkirov, Param. Reson. Colloq., Kazan (1960) p. 54.
[37]J. H. Van Vleck, *The Theory of Electric and Magnetic Susceptibilities* (Oxford U. P. London, 1932) p. 275.
[38]E. J. W. Verwey, P. W. Haayman, and F. C. Romeijn, J. Chem. Phys. 15, 181 (1947).
[39]Reference 1, p. 156.
[40]Reference 1, p. 197 and (private communication).
[41]P. W. Anderson, Phys. Rev. Lett. 34, 953 (1975).
[42]I. G. Austin and N. F. Mott, Adv. Phys. 19, 41 (1969).
[43]Reference 1, p. 76.